The fate of a graphene flake: a new route towards fullerenes disclosed with ab initio simulations

Fabio Pietrucci and Wanda Andreoni*

Institute of Theoretical Physics

Ecole Polytechnique Fédérale de Lausanne, Switzerland

E-mail: fabio.pietrucci@epfl.ch;wanda.andreoni@epfl.ch

SUPPORTING INFORMATION

Methods and computational details

A.

All calculations employed the CPMD code [1] and relied on the following scheme: the Perdew-Burke-Ernzerhof (PBE) approximation for the exchange-correlation functional,[2] norm-conserving pseudopotentials constructed with the Martins-Trouiller procedure ,[3] and a plane-wave basis set up to a cutoff of 50 Ry. Periodic boundary conditions were applied: a cubic unit cell of 20Å edge for the 60- and 62-atom flakes, a orthorhombic one 24x18x18 Å^3 for the 68-atom ribbon. The artificial periodic images were decoupled using the Hockney's Poisson solver.[4]

The Car-Parrinello[5] MD runs used a time step of 0.096 fs (up to T=1000 K) or 0.048 fs (above T=1000 K) for the integration of the equation of motion using the Verlet algorithm, and a fictitious mass 900 a.u for the electronic degrees of freedom. Simulations were carried out both at

*To whom correspondence should be addressed

300 K, 1000 K, 2000 K and 3000 K, using the Nosé-Hoover algorithm,[6,7] for a cumulative length of more than 800 ps. In the MTD runs, in order to prevent deviations connected with the metadynamics bias, the wavefunctions were "quenched" to the Born-Oppenheimer surface every 250 fs. Wavefunction optimization was performed with the preconditioned conjugate-gradients method. Geometry optimization used the L-BFGS method.[8]

B.

MTD was driven by the PLUMED[9] plugin interfaced with CPMD .[1] Our strategy consisted of two different MTD series of simulations, using different collective variables (CVs): first, in order to discover transformation mechanisms without making any assumption about the pathways and products, we employed the social permutation invariant topological (SPRINT) coordinates;[10] then, for selected reactions thus identified, and using the SPRINT-MTD pathway as reference, we applied the path-CVs [11] to characterize the transition state more precisely and to estimate the corresponding free-energy barrier with higher accuracy. Full consistency was found between the results obtained when using one or the other set of collective variables.

The SPRINT coordinates are defined as

$$S_i = \sqrt{N}\lambda^{\max} v_i^{\max,\text{sorted}} ; \quad i = 1,2,...,N \tag{1}$$

where N is the number of atoms, $\lambda^{\max}$ and $v_i^{\max,\text{sorted}}$ are the largest eigenvalue and corresponding eigenvector (with sorted entries) of the adjacency matrix of atoms

$$a_{ij} = \frac{1-(r_{ij}/r_0)^n}{1-(r_{ij}/r_0)^m} , \tag{2}$$

where r_{ij} are interatomic distances and r_0, n, and m are parameters depending on the typical bond-lengths of the system under consideration. For carbon, we used r_0 = 2 Å, n = 8, m = 16.

We emphasize that, although all carbon atoms entered the above definitions, we could benefit from the dimensional reduction allowed by the magnitude-ordering, which introduces correlations among the values of the S_is. Only seven out of them were biased for each system. Hills were

deposited every 50 fs along the trajectory, with heights of 0.016 eV or 0.011 eV for the nanoflake simulations and 0.027-0.1 eV for the nanoribbon simulations, and a width of 0.7-1.2 in all cases.

The cartesian distance D between distance matrices d_{ij} was chosen as metric for the definition of the path CVs (s,z)[11] :

$$s = \frac{1}{Z}\sum_{\alpha} \alpha\, e^{-\lambda D^2(d_{ij},d_{ij}^{\alpha})} \tag{3}$$

and

$$z = -\lambda^{-1}\log Z \tag{4}$$

with

$$Z = \sum_{\alpha} e^{-\lambda D^2(d_{ij},d_{ij}^{\alpha})} \tag{5}$$

where the index α spans the configurations included in the reference path, and λ is chosen so that $\lambda D^2(d_{ij}^{\alpha}, d_{ij}^{\alpha+1}) \approx 1$. s measures the progress along the path and z the distance from the path.

The reference path was defined via sixteen frames extracted from the SPRINT-driven trajectory spanning the desired transformation. Depending on the reaction investigated, different sets of atoms were included in the definition of the CVs. Hills of height 0.027 eV and width 0.2 were added along the trajectory every 100 fs.

C.

A plot of the energy as a function of time is not informative in our simulations. Only in some cases it allows to spot out locally stable structures (in the form of local energy minima), but in many cases it is too noisy. The reason is that the simulation is performed at relatively high temperature (1000K), and in addition the history-dependent bias of metadynamics perturbs the energy profile. This is a major difference from traditional methods aimed only at finding local energy minima, like simulated annealing, genetic algorithm or minima hopping, and for which the (potential) energy landscape is relevant.

Edge reconstruction of a graphene nanoribbon

We apply our strategy to the study of a well-known transformation of a graphene-related structure: the (66) to (57) reconstruction at the zigzag edges of a graphene nanoribbon (GNR).[12] The motivation is twofold: these calculations can be considered as a further validation of the SPRINT-MTD method as prejudice-free approach and also as a reference for the energy scale of the structural transitions leading to the closed cage. Having such a reference is useful because there is no experimental determination of activation or isomerization energies and also because relative values of quantities like barriers are less dependent than the absolute values on the exchange-correlation functional.

We considered the structural evolution of a 68-atom GNR including two zigzag and two armchair edges (see Figure 1). Our SPRINT search, both at 300 K and 1000 K, showed that the early transformations occurring in the structure of the planar fragment were the (66) to (57)-reconstructions of the zigzag edges, in full agreement with the HRTEM observations [12] and their interpretation based on DFT calculations.[13,14] While the reshaping of zigzag edges propagated, the armchair edges remained unchanged.

Subsequent path-metadynamics resulted in a free-energy barrier of 0.9 eV for the first reconstruction at room temperature, and a sizably reduced value, of 0.5 eV, for the adjacent (66) to (57) transformation. These results are consistent with previous calculations based on predefined pathways: a 0.6 eV barrier at T=0K for the first transition, obtained with nudged-elastic-band calculations,[13,14] and a 0.83 eV free-energy-barrier at room temperature, from Montecarlo and umbrella sampling simulations using a well-tuned carbon potential .[15]

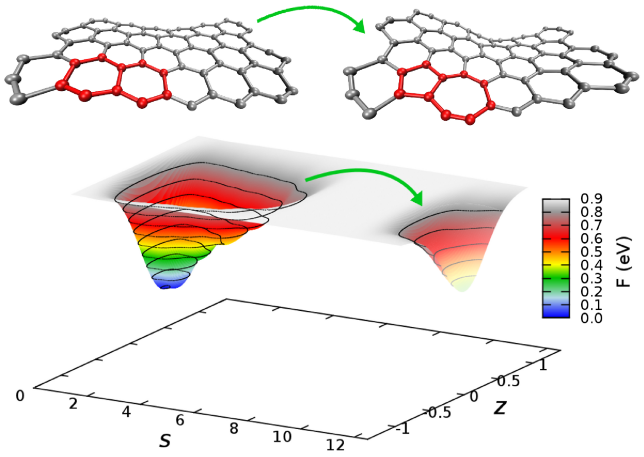

Figure 1: Graphene nanoribbon: (66) to (57) reconstruction of the zigzag edge and free-energy landscape as a function of the path collective variables, at room temperature.

More supporting results

Results of the unbiased MD following the closing of the cage are illustrated in Figure 2.

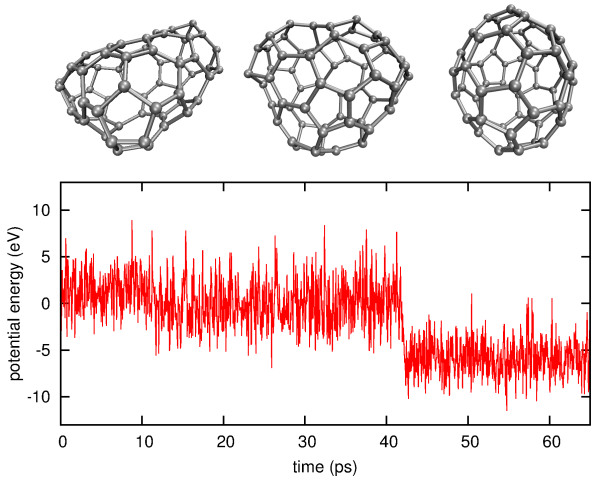

Figure 2: Reshaping of the carbon cage: variation of the potential energy during an unbiased CPMD simulation at 3000K.

The tendency to edge zipping can be deduced from the electron-localization-function (ELF)[16] illustrated in Figure 3(a). Thus early step is accompanied by the formation of the carbon square (Figure 3(b)).

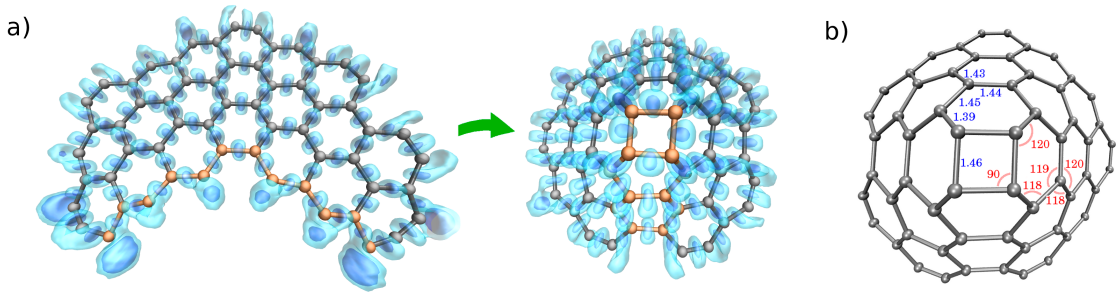

Figure 3: a) Electron localization function (ELF): from the nanoflake to the nanocone, showing the disappearance of the dangling bonds (isovalues = 0.78; 0.88); b) Geometrical characterization of the nanocone, with bondlengths in Å and angles in degrees.

In the 1000K simulation sketched in Figure 1(c) of the main text, the C_2 unit is expelled from the nanocone, bearing sufficient kinetic energy to overcome the attractive interaction with C_{58}. After a short time interval (2.6 ps) it is recaptured. We have observed that periodic boundary conditions facilitate this event. Figure 4 shows indeed that, during this time the motion of C_2 becomes

ballistic and crosses a few times the box boundaries. The ballistic nature of the C_2 motion is made possible at distances where the interaction between the two molecules becomes very weak. As a confirmation, we computed the total energy difference ΔE between one of these configurations, with C_2 at 7 Å and 7.2 Å from C_{58}, differing only for a rigid relative translation. The energy difference is only 0.005 eV (to be compared with the thermal energy of 0.08 eV), corresponding to a force of only 0.025 eV / Å . One may wonder about the strength of Van der Waals interactions in these geometries and whether including them would have changed our conclusions. Therefore, we repeated the calculation including Grimme's D2 dispersion corrections [17,18] to the PBE functional. The total energy difference ΔE amounted to 0.0001 eV, corresponding to a force of only 0.0005 eV/ Å between C_2 and C_{58}. Of course, if the C_2 unit would detach with a smaller kinetic energy, it could be recaptured sooner, without the help of the periodic boundary conditions. As far as the "comeback" is soft, how this happens does not change the progress of the structural transformation.

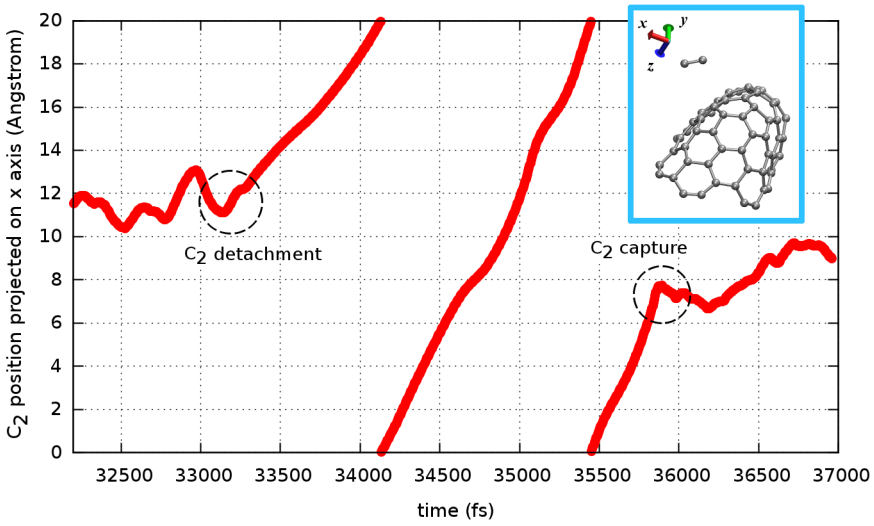

Figure 4: Position of the center of mass of C_2, projected along the x axis, as a function of time.

References

(1) CPMD, Copyright IBM Corp. 1990-2014, Copyright MPI für Festkörperforschung Stuttgart 1997-2001, http://www.cpmd.org.

(2) Perdew, J. P.; Burke, K.; Ernzerhof, M. *Phys. Rev. Lett.* **1996**, *77*, 3865–3868.

(3) Troullier, N.; Martins, J. L. *Phys. Rev. B* **1991**, *43*, 1993–2006.

(4) Hockney, R. W. *Methods Comput. Phys.* **1970**, *9*, 136–211.

(5) Car, R.; Parrinello, M. *Phys. Rev. Lett.* **1985**, *55*, 2471–2474.

(6) Nosé, S. *J. Chem. Phys.* **1984**, *81*, 511–519.

(7) Hoover, W. *Phys. Rev. A* **1985**, *31*, 1695–1697.

(8) Billeter, S.; Curioni, A.; Andreoni, W. *Comput. Mat. Sci.* **2003**, *27*, 437–445.

(9) Bonomi, M.; Branduardi, D.; Bussi, G.; Camilloni, C.; Provasi, D.; Raiteri, P.; Donadio, D.; Marinelli, F.; Pietrucci, F.; Broglia, R. A.; Parrinello, M. *Comp. Phys. Comm.* **2009**, *180*, 1961–1972.

(10) Pietrucci, F.; Andreoni, W. *Phys. Rev. Lett.* **2011**, *107*, 085504–085507.

(11) Branduardi, D.; Gervasio, F. L.; Parrinello, M. *J. Chem. Phys.* **2007**, *126*, 054103–054112.

(12) Girit, C. O.; Meyer, J. C.; Erni, R.; Rossell, M. D.; Kisielowski, C.; Yang, L.; Park, C.-H.; Crommie, M. F.; Cohen, M. L.; Louie, S. G.; Zettl, A. *Science* **2009**, *323*, 1705–1708.

(13) Koskinen, P.; Malola, S.; Häkkinen, H. *Phys. Rev. Lett.* **2008**, *101*, 115502–115505.

(14) Koskinen, P.; Malola, S.; Häkkinen, H. *Phys. Rev. B* **2009**, *80*, 073401–073403.

(15) Kroes, J. M. H.; Akhukov, M. A.; Los, J. H.; Pineau, N.; Fasolino, A. *Phys. Rev. B* **2011**, *83*, 165411–165418.

(16) Savin, A.; Nesper, R.; Wengert, S.; Faessler, T. F. *Angew. Chem. Int. Ed. Engl.* **1997**, *36*, 1808–1832.

(17) Grimme, S. *J. Comput. Chem.* **2004**, *25*, 1463–1473.

(18) Grimme, S. *J. Comput. Chem.* **2006**, *27*, 1787–1799.